Journal of Advanced Research 47 (2023) 27–40

Contents lists available at ScienceDirect

Journal of Advanced Research

journal homepage: www.elsevier.com/locate/jare

Original Article

Beet cyst nematode HsSNARE1 interacts with both AtSNAP2 and AtPR1 and promotes disease in Arabidopsis

Jie Zhao, Shiming Liu *

State Key Laboratory for Biology of Plant Diseases and Insect Pests, Institute of Plant Protection, Chinese Academy of Agricultural Sciences, Beijing 100193, PR China

HIGHLIGHTS

- A *t*-SNARE domain-containing effector HsSNARE1 was identified from beet cyst nematode (BCN).
- Protein structure modeling analysis found that three mutations (E141D, A143T and −148S) altered regional structure of HsSNARE1 from random coils to α-helixes.
- Expression of *HsSNARE1* significantly enhanced while expression of its highly homologous soybean cyst nematode (SCN) HgSNARE1 and its mutant *HsSNARE1-M1*, both of which carry those above-mentioned three mutations, remarkably suppressed BCN susceptibility of Arabidopsis.
- HsSNARE1 promotes cyst nematode disease by interaction with both AtSNAP2 and AtPR1 via its *t*-SNARE domain and *N*-terminal uncharacterized fragment, respectively, and significant suppression of both *AtSHMT4* and *AtPR1*.
- This work pinpoints a new molecular mode of action of the *t*-SNARE-domain containing cyst nematode effectors.

GRAPHICAL ABSTRACT

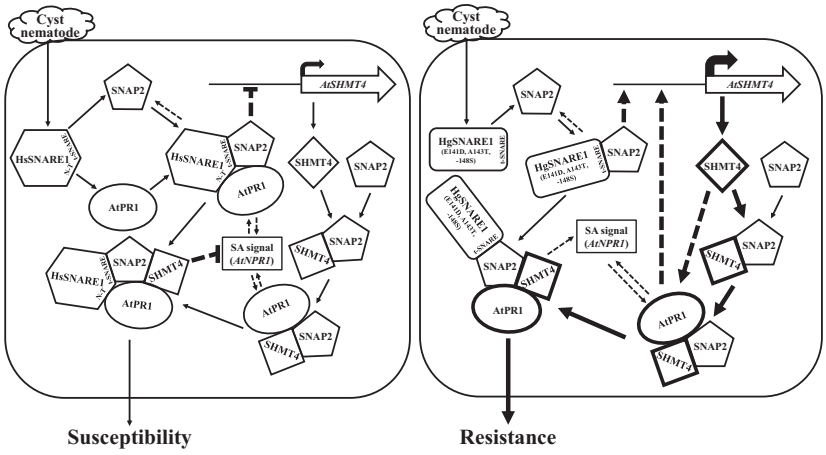

ARTICLE INFO

Article history:
Received 16 May 2022
Revised 29 June 2022
Accepted 17 July 2022
Available online 22 July 2022

Keywords:
Cyst nematodes
t-SNARE proteins

ABSTRACT

Introduction: Plant parasitic cyst nematodes secrete a number of effectors into hosts to initiate formation of syncytia and infection causing huge yield losses.
Objectives: The identified cyst nematode effectors are still limited, and the cyst nematode effectors-involved interaction mechanisms between cyst nematodes and plants remain largely unknown.
Methods: The *t*-SNARE domain-containing effector in beet cyst nematode (BCN) was identified by *In situ* hybridization and immunohistochemistry analyses. The mutant of effector gene was designed by protein structure modeling analysis. The functions of effector gene and its mutant were analyzed by genetic transformation in Arabidopsis and infection by BCN. The protein–protein interaction was analyzed by

Peer review under responsibility of Cairo University.
* Corresponding author.
E-mail address: liushiming01@caas.cn (S. Liu).

https://doi.org/10.1016/j.jare.2022.07.004

AtSNAP2
AtPR1
Interaction
Disease

yeast two hybrid, BiFC and pulldown assays. Gene expression was assayed by quantitative real-time PCR.
Results: A *t*-SNARE domain-containing BCN HsSNARE1 was identified as an effector, and its mutant HsSNARE1-M1 carrying three mutations (E141D, A143T and −148S) that altered regional structure from random coils to α-helixes was designed and constructed. Transgenic analyses indicated that expression of *HsSNARE1* significantly enhanced while expression of *HsSNARE1-M1* and highly homologous *HgSNARE1* remarkably suppressed BCN susceptibility of Arabidopsis. HsSNARE1 interacted with AtSNAP2 and AtPR1 via its *t*-SNARE domain and *N*-terminal, respectively, while HsSNARE1-M1/HgSNARE1 could not interact with AtPR1 but bound AtSNAP2. AtSNAP2, AtSHMT4 and AtPR1 interacted pairwise, but neither HsSNARE1 nor HsSNARE1-M1/HgSNARE1 could interact with AtSHMT4. Expression of *HsSNARE1* significantly suppressed while expression of *HsSNARE1-M1/HgSNARE1* considerably induced both *AtSHMT4* and *AtPR1* in transgenic Arabidopsis infected with BCN. Overexpression of *AtPR1* significantly suppressed BCN susceptibility of Arabidopsis.
Conclusions: This work identified a *t*-SNARE-domain containing cyst nematode effector HsSNARE1 and deciphered a molecular mode of action of the *t*-SNARE-domain containing cyst nematode effectors that HsSNARE1 promotes cyst nematode disease by interaction with both AtSNAP2 and AtPR1 and significant suppression of both *AtSHMT4* and *AtPR1*, which is mediated by three structure change-causing amino acid residues.

Introduction

Plant parasitic cyst nematodes (Heterodera and Globodera) are sedentary endoparasites of plant roots and the primary nematode pathogens of most crop species worldwide. Cyst nematodes secrete many effectors into their hosts for initiating the formation of feeding sites (syncytia) and for completing their whole life cycle in the plant roots. The cyst nematode effectors are mainly secreted into plant cells by esophageal gland via stylet, while one part of effectors are secreted into plant cells by cuticle or amphid [1–4]. A number of cyst nematode effectors have been identified, and they play various vital roles in the parasitism. Some nematode effectors such as HsCBP, a cellulose binding protein [5], 19C07 [6] and B-type CLE peptides [7] can function in loosening and/or degrading and modifying cell wall, and in inducing the formation and development of feeding sites, while some other nematode effectors such as Hg10A06 [8], 30C02 [9] and GLAND18 [10] can suppress the defense reactions of plants and/or regulate the gene expression of host plants, and the nuclear effector GLAND4 functioned to have the DNA-binding ability [11]. Cyst nematodes could even synthesize and secrete hormone cytokinins into plants to mediate the cell divisions and feeding site formation [12]. Meanwhile, progress has been achieved in the detailed molecular modes of action of cyst nematode effectors in the hosts. The effector 10A07 interacted with IPK (interacting plant kinase) and IAA6 transcription factor, IPK phosphorylated 10A07 to mediate its translocation from cytoplasm to nucleus and promote the parasitism [13]. The nematode effector 25A01 could interact with various plant proteins such as an Arabidopsis F-box-containing protein, a chalcone synthase and the translation initial factor eIF-2bs to promote the susceptibility to nematodes [14]. The effector 30D08 interacted with SMU2, an auxiliary spliceosomal protein, to likely alter the pre-mRNA splicing and regulate the gene expression [15]. The effector 4E02 targets the vacuolar cysteine protease RD21A in Arabidopsis and mediates its transport from vacuoles to the nucleus and cytoplasm, thus interfering with carbohydrate metabolism and inhibiting the defense response of host plants [16]. Two SCN effectors, 2A05 (Hg-VAP2) and 7E05 can interact with soybean Bcl-2 associated anthanogene 6 (GmBAG6-1) to inhibit cell death induced by GmBAG6-1 [17].

SNARE (soluble NSF attachment protein receptor) proteins are a superfamily characterized by the presence of specific SNARE domains [18]. SNARE proteins are classified into Qa-, Qb-, Qc-, SNAP25-like, and R-SNAREs, based on the conserved amino acids of SNARE motifs with coiled-coil helices [19,20]. The SNARE proteins can mediate the fusion between vesicular and target membranes. Many studies have shown that the plant SNARE domain-containing proteins play a vital role in the defense of plants against parasitic nematodes. The R-SNARE VAMP727 and Qa-SNARE SYP22 regulated Arabidopsis defense against root-knot nematodes (RKNs) by interacting with the plasma membrane (PM)-bound receptor BRASSINOSTEROID INSENSITIVE1 (BRI1) to control BRI1 intracellular trafficking [21,22]. In soybean, the resistant-type *rhg1* α-SNAP (soluble NSF attachment protein, GmSNAP18) would be abnormally accumulated in the feeding sites of soybean cyst nematode (SCN, *Heterodera glycines*) and show cytotoxicity to interrupt the SNARE complexes and vesicular trafficking when SCN infects soybean, such might result in resistance to SCN [23]. However, the soybean NSF_{RAN07} (*N*-ethylmaleimide-sensitive fusion protein, Glyma.07 g195900) could strongly bind and balance the cytotoxicity of *rhg1* α-SNAP by destroying SNARE complex circulation to ensure the normal growth of plants [24]. Recently, two *t*-SNARE domain-containing soybean syntaxins (Glyma.12 g194800 and Glyma.16 g154200) were identified to strongly bind *rhg1-b* α-SNAP (*rhg1-b* GmSNAP18) and mediate resistance of *rhg1-b* to SCN [25]. An α-SNAP-interacting protein GmSYP31A (Glyma.02 g255700), a Qa-SNARE protein in soybean, was characterized to be involved in regulation of VDAC-mediated mitochondrial membrane potential, and to induce SCN resistance of soybean by activating cell death at the feeding sites [26].

However, the functions and mechanisms of SNARE domain-containing proteins of cyst nematodes in the parasitism were seldom reported. A *t*-SNARE domain-containing gene *HgSLP-1* was identified in SCN by allelic imbalance analysis, and HgSLP-1 could physically interact with soybean *rhg1-a* GmSNAP18 (*rhg1-a* α-SNAP), which underlies SCN resistance in Peking-type soybeans [27], but it was not yet functionally characterized. The main objectives of this study were to identify the *t*-SNARE domain-containing proteins from cyst nematodes (SCN and beet cyst nematode (BCN) *Heterodera schachtii*) that can act as the effectors, and to functionally characterize the molecular modes of their actions using the Arabidopsis-BCN compatible interaction system. In this study, a SNARE domain-containing effector HsSNARE1 was identified in BCN, with comparison to the actions of its mutant HsSNARE1-M1 and its highly homologous HgSNARE1 identified in SCN, a novel molecular mechanism of effectors promoting nematode disease was deciphered by HsSNARE1 directly interacting with both an α-SNAP (AtSNAP2) and a pathogenesis-related protein AtPR1 and significantly suppressing the expression of *AtSHMT4* and *AtPR1* in Arabidopsis.

Materials and methods

Cyst nematodes and plant materials

SCN HG Type 1.2.3.5.7 (race 4) was used in this study and propagated on soybean cultivar 'Zhonghuang 13' that is susceptible to SCN [28]. BCN was propagated on beets (*Beta vulgaris* L.). Arabidopsis Col-0 was used as the wild-type Arabidopsis that can be infected by BCN.

In-situ hybridization

In-situ hybridization was carried out using pre-parasitic J2s (pre-J2s), the specific primers of *HsSNARE1* were used to synthesize digoxigenin (DIG)-labelled sense and antisense cDNA probes (Roche, Germany), the fixation, hybridization, color rendering all were performed as described [29,30]. Observation was performed and pictures were captured under an Olympus BX53 upright microscope (Olympus, Tokyo, Japan).

Gene expression analysis

Regarding the expression of *HsSNARE1* in nematodes, the pre-parasitic J2s (pre-J2s) of BCN were hatched at 28 ℃ in the dark. The parasitic BCN juveniles and adults at different stages were isolated with the method described by Elling et al. [31]. As for the expression of *AtSNAP2*, *AtSHMT4*, *AtPR1* and *AtNPR1* in Arabidopsis, each Arabidopsis seedling was inoculated with 300 BCN J2s. Roots were collected at 0 h, 24 h, 36 h, and 5 d post inoculation (hpi/dpi), respectively. The mRNA was extracted using approximately 1,000 nematodes at different stages, or from the collected Arabidopsis roots at different time-frame points employing the Dynabeads mRNA DIRECT kit (Invitrogen, Vilnius, Lithuania), and the cDNA was synthesized using the PrimeScript™ RT reagent kit with gDNA Eraser kit (Takara, Kusatsu, Japan). Quantitative real-time PCR (qRT-PCR) reaction solutions were prepared using the TB Green™ Premix Ex Taq™ (Tli RNaseH Plus) kit (Takara, Kusatsu, Japan), and qRT-PCR was conducted on a 7500 Fast Real-Time PCR system (Applied Biosystems, USA). *HsActin* and *AtActin* were used as the reference genes for the expression of nematode and Arabidopsis genes, respectively. The corresponding primers were listed in Table S1. The relative expression was calculated relative to the expression level in the nematode eggs or in the wild-type Col-0 at 0 hpi by the $2^{-\Delta\Delta Ct}$ method [32]. Three replicates were set each time for these experiments, and the experiments were replicated thrice. The significant difference of *HsSNARE1* expression in nematodes was statistically analyzed by Duncan's multiple range test ($P < 0.05$), and the significant difference of gene expression in the transgenic Arabidopsis relative to in the wild-type Col-0 at the same time-frame point was statistically analyzed by one-way ANOVA method, using SPSS version 25 software (IBM, Armonk, NY, USA).

Nematode immunolocalization analysis

Anti-HsSNARE1 antibody was generated using 1-210th amino acid residues of HsSNARE1 at ABclonal (Wuhan, China). Western blotting was conducted to test the specificity. Immunolocalization assay was done using BCN pre-parasitic J2s by the method of Zhao et al. [33]. The final anti-HsSNARE1 antibody concentration was quantified to 10 μg/mL, and then FITC-labeled Goat Anti-Rabbit IgG (H + L) (1:300) (Beyotime Institute of Biotechnology, Haimen, Jiangsu, China) was used for immunofluorescence staining. In the end, the fluorescence was observed using a Zeiss LSM 980 laser confocal microscope (Zeiss, Jena, Germany).

Plant immunohistochemistry analysis

Two-week-old beet seedlings were inoculated with pre-parasitic BCN J2s. At 7 dpi, the root sections containing BCN feeding sites were collected, and then dissected into small pieces. The process of tissue fixation, dehydration, osmosis and rehydration were conducted as describe by Zhao et al. [33]. In a brief, the tissues were placed in 8 % paraformaldehyde, vacuumed and fixed at 4 ℃ for one week. After dehydration with gradient ethanol (15 %, 30 %, 50 %, 70 %, 85 %, and 100 %) on ice, the tissues were immersed in 100 % butylmethylmethacrylate for at least 1 week. The samples were placed in an embedded box containing 100 % methacrylate + 0.5 % benzoin ethyl ether + 1 mM dithiothreitol and polymerized under UV for at least 4 h. The sections were incubated in acetone for 1 h to remove butylmethylmethacrylate. Sections were incubated with anti-HsSNARE1 antibody (5 μg/mL) at 4 ℃ overnight in a damp box. Finally, slides were incubated with FITC-labeled Goat anti-Rabbit IgG (H + L) (1:300) (Beyotime Institute of Biotechnology, Haimen, Jiangsu, China). Observation was performed under a Zeiss LSM 980 laser confocal microscope (Zeiss, Jena, Germany).

Subcellular localization analysis

HsSNARE1 was amplified using the corresponding primers listed in Table S1 and cloned into pYBA1132 fused with a GFP at the C-terminus. By the method of Luo et al. [34], the plasmid including the empty vector pYBA1132 was transformed into *Agrobacterium tumefaciens* EHA105 competent cells to prepare *Agrobacterium* suspensions, and the suspensions were then injected into *Nicotiana benthamiana* leaves using a 1 ml syringe. At 36–48 hours post injection, the fluorescence is observed under a Zeiss LSM 980 laser confocal microscope (Zeiss, Jena, Germany). The GFP fluorescence signals were excited at 488 nm, and collected at 505–550 nm.

Arabidopsis transformation

HsSNARE1, *HgSNARE1*, and *HsSNARE1-M1* were cloned into pH7WG2D with a *CaMV35S* promoter by the Gateway method using Gateway BP Clonase™ II Enzyme Mix kit (Invitrogen, Carlsbad, USA). *AtPR1* was cloned into pDT7 with a *Bar* tag to construct pDT7:*AtPR1*.The constructs were transformed into *Agrobacterium tumefaciens* GV3101. The Arabidopsis transformation was performed by the flower bud soaking method [35]. The transformed seedlings were drained a little, and grew for 24 h in the dark and then under the normal growth conditions. The harvested seeds were screened on the 1/2 MS medium with hygromycin or basta to obtain positive seedlings. The positive seedlings were further identified by RT-PCR using the corresponding primers listed in Table S1, and the seeds were harvested from the positive plants. Following progeny test, the homozygous T2 generation plants were used for the phenotyping and gene expression measurement.

Phenotyping Arabidopsis infected with BCN

Eight identified homozygous transgenic Arabidopsis lines expressed with *HsSNARE1* (HsSNARE1-1 and HsSNARE1-2), *HgSNARE1* (HgSNARE1-1 and HgSNARE1-2), *HsSNARE1-M1* (HsSNARE1-M1-1 and HsSNARE1-M1-2), or *AtPR1* (AtPR1-OE-1 and AtPR1-OE-2), respectively (Figure S7) were phenotyped with the infection of BCN by the method [5] with some modifications. Briefly, the wild-type and transgenic Arabidopsis seeds first germinated on the 1/2 MS medium following seed sterilization, about one week after germination, the seedlings were transplanted into the plastic cups filled with sand and soil (7:3, w/w) and grew for 3–4 weeks at 24 ℃ under 16 h/8h light/dark. Then, each seedling was inoculated with 300 hatched J2s. The samples including the

seedlings and soils were collected at different dpi to observe and the BCN at each developmental stage (J2, J3, J4, female and cyst) was counted under an Olympus SE61 stereomicroscope (Japan). The experiments were carried out independently thrice with at least 6 replicates each line each time. The significant difference was statistically analyzed by one-way ANOVA using SPSS version 25 software (IBM, Armonk, NY, USA).

Modeling of SNARE domain-containing cyst nematode proteins

The Phyre 2 (https://www.sbg.bio.ic.ac.uk/phyre2/html/page.cgi?id = index) was employed to perform the modeling and analyze the structure of cyst nematode *t*-SNARE domain-containing proteins HsSNARE1 and HgSNARE1.

Yeast two hybrid assay

The cDNAs of *HgSNARE1* and *HsSNARE1* were amplified using SCN HG Type 1.2.3.5.7 (race 4) and BCN cDNA, respectively, using the primers listed in Table S1 and then cloned into pGADT7 using the ClonExpress II One Step Cloning kit (Vazyme, Nanjing, China). In the same way, *HsSNARE1*$^{1\text{-}729/730\text{-}933/934\text{-}1032}$ fragments were cloned into pGADT7. *AtSNAP2* (*AT3G51690*) was cloned into pGBKT7 to obtain pGBKT7:*AtSNAP2*, which was then transformed into *Saccharomyces cerevisiae* strain Y2H Gold using the Matchmaker Gold Yeast Two-Hybrid System (Takara, Mountain View, USA) and used as the bait. Their interactions were performed by yeast two hybrid assay following the instruction of Matchmaker Gold Yeast Two-hybrid User Manual (https://www.clontech.com).

BiFC assay

The *AtSNAP2*, *AtSHMT4* and *AtPR1* were cloned into pSPYNE(R)173 to generate pSPYNE(R)173:*AtSNAP2*, pSPYNE(R)173:*AtSHMT4*, and pSPYNE(R)173:*AtPR1*. *HgSNARE1*, *HsSNARE1*, *HsSNARE1*$^{1\text{-}729}$, *HsSNARE1*$^{730\text{-}933}$, *HsSNAR1-M1*, *AtSHMT4* and *AtPR1* were cloned into pSPYCE(M) to generate pSPYCE(M):*HgSNARE1*, pSPYCE(M):*HsSNARE1*, pSPYCE(M):*HsSNARE1*$^{1\text{-}729}$, pSPYCE(M):*HsSNARE1*$^{730\text{-}933}$, pSPYCE(M):*AtSHMT4*, pSPYCE(M):*AtPR-1*, and pSPYCE(M):*HsSNARE1-M1*, respectively. The primers were listed in Table S1. As described by Luo et al. [34], the constructs were transformed into *Agrobacterium tumefaciens* EHA105 to prepare *Agrobacterium* suspensions, which were then injected into *Nicotiana benthamiana* leaves using a 1 ml syringe. About 2–3 days after injection, the fluorescence was observed under a Zeiss LSM 880 laser confocal microscope (Zeiss, Jena, Germany). OsHAK5 (Os1g0930400) and Hg15982 (Hetgly.T000015982.1, a C_2H_2-type zinc finger protein of SCN *Heterodera glycines*) were used as the negative controls.

Pulldown assay

The bait proteins and target proteins were respectively cloned into pGEX-4T-1 and pET-32a to express GST- and His-fusion proteins in *E. coli* strain BL21 Gold (DE3). The fusion proteins were expressed and purified by the method [36]. The proteins were induced by adding 0.5 mM isopropylthio-β-Dgalactopyranoside (IPTG, Sigma) at 16 ℃ for 16 h, and the GST- fusion proteins were purified using a glutathione (GST) agarose affinity chromatography column (Glutathione Sepharose 4B, GE Healthcare, Sweden), while His-fusion proteins were purified using a histidine-labeled affinity chromatography column (Ni Sepharose HP, GE Healthcare, Sweden). GST-mediated pulldown assay was performed as described by the method [36]. The GST- fusion proteins were separately mixed with His-fusion proteins by 3:1 and then incubated with the prewashed glutathione (GST) beads at 4 ℃ overnight. The pGEX-4T-1 expressed with His-fusion proteins were used as the negative control. The bound proteins were eluted and mixed with SDS loading buffer, boiled, and then analyzed using SDS-PAGE and immunoblotting with a GST-Tag Mouse mAb (ABclonal, Wuhan, China) and a His-Tag Mouse mAb (ABclonal, Wuhan, China).

Results

Identification of a t-SNARE domain-containing BCN effector HsSNARE1

The genome of SCN 'TN10' has been sequenced as the reference genome of SCN [37] and its genome and transcriptome databases are available (https://www.scnbase.org). A *t*-SNARE domain-containing gene *HgSLP-1* (GenBank Acc. No.: KM575849) has been isolated from SCN [27]. In this study, according to the reference transcriptome of SCN 'TN10' (Heterodera Glycines V1 CDS), another *t*-SNARE domain-containing gene was isolated from SCN HG Type 1.2.3.5.7 (race 4) [28]. This isolated gene showed three SNPs (single nucleotide polymorphisms) different from *Hetgly. T000011771.1* in the cDNA sequence with only one amino acid alteration in the predicted protein sequence. This gene is 1035 bps in length containing an uncharacterized fragment (1–732 bps) in the *N*-terminal, one *t*-SNARE domain (733–936 bps) and one transmembrane (TM) domain (970–1023 bps) in the C-terminal (Figure S1). The predicted protein sequence encoded by this gene is significantly different from that of HgSLP-1 (Figure S2). We named this gene as *HgSNARE1* hereafter. Afterwards, while using the same set of primers to conduct PCR-amplification employing the cDNA of BCN, we obtained a homologous gene with similar gene structure, which encodes a protein with 96.8 % of similarity to HgSNARE1 (Figure S3). We hereafter named this gene as *HsSNARE1*.

Subsequently, HsSNARE1 was selected for characterization. The *in-situ* hybridization analysis indicated that the transcripts of *HsSNARE1* was specifically accumulated in the subventral gland in BCN (Fig. 1A, S4). The immunolocalization analysis verified that HsSNARE1 was localized in the subventral gland of nematodes (Fig. 1B, S5). The qRT-PCR analysis showed that *HsSNARE1* was mainly expressed at the J3 (J3) stage, and then at the parasitic J2 (Par-J2) stage (Fig. 1C). Subsequently, the localization of HsSNARE1 in plants was analyzed after BCN infection. The immunolocalization results indicated that HsSNARE1 was secreted into cells of roots of beet seedlings (Fig. 1D, S6). All these results indicate that HsSNARE1 acted as an effector. Furthermore, the transient analysis showed that HsSNARE1 was localized on the plasma membrane and in the nucleus of cells of *Nicotiana benthamiana* leaves (Fig. 1E).

Opposite functions of HsSNARE1 and HgSNARE1 in susceptibility of transgenic Arabidopsis to BCN

Three SNARE domain-containing soybean syntaxins mediate the SCN resistance [25,26]. To understand the impact of the *t*-SNARE domain-containing cyst nematode genes on the responses of plants to nematodes, the transgenic lines expressed with either *HsSNARE1* or *HgSNARE1* were generated using wild-type Arabidopsis Col-0 (Figure S7A, B), and the homozygous T2 transgenic Arabidopsis seedlings were inoculated with BCN.

As for the *HsSNARE1*-expressed Arabidopsis, at 35 days post inoculation (dpi), the cysts per plant were significantly increased in both identified homozygous transgenic lines (HsSNARE1-1 and HsSNARE1-2), compared to wild-type Col-0 ($P < 0.01$ in HsSNARE1-1 and $P < 0.0001$ in HsSNARE1-2, Fig. 2A). The obtained results indicate that expression of *HsSNARE1* enhanced the susceptibility of Arabidopsis to BCN.

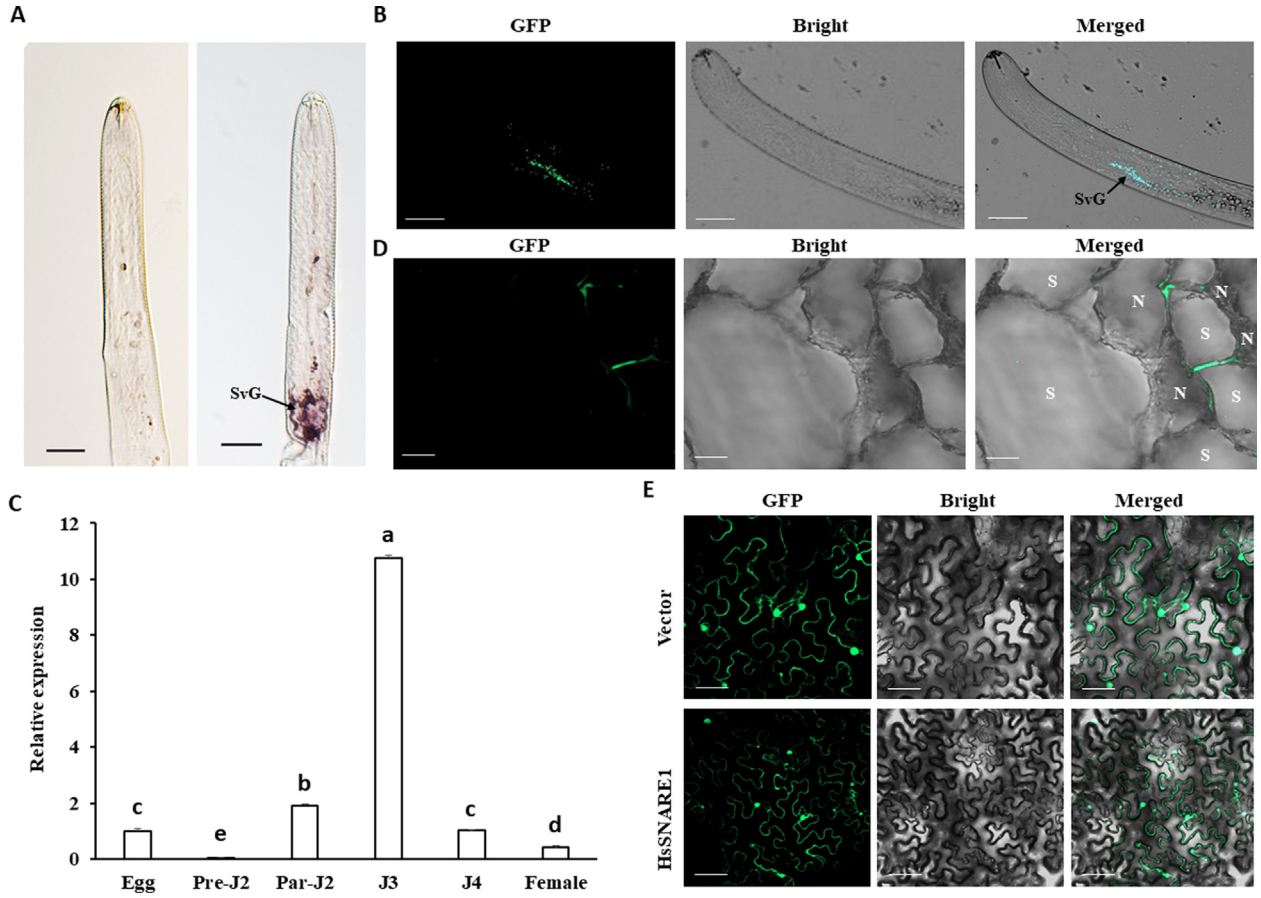

Fig. 1. Localization and temporal expression pattern of HsSNARE1. (A) *In-situ* hybridization with the HsSNARE1 sense probe (left) and digoxigenin-labelled anti-sense probe (right) to pre-parasitic second-stage BCN juveniles (J2s) Bar=50μm. (B) Immunolocalization of HsSNARE1 in pre-parasitic BCN J2s using anti-HsSNARE1 antibody Bar=20μm. (C) Temporal expression pattern of *HsSNARE1* in BCN. The relative expression was quantified for each nematode stage relative to the egg stage. Pre, pre-parasitic; Par, parasitic; J, juvenile. Different letters represent statistically significant difference by Duncan's multiple range test ($P < 0.05$). (D) Immunolocalization of HsSNARE1 in beet seedling roots using anti-HsSNARE1 antibody. S, syncytium; N, nematode Bar=10μm. (E) Subcellular localization of HsSNARE1 in *Nicotiana benthamiana* cells by transient expression Bar=20μm. The GFP fluorescence signals were excited at 488 nm, and collected at 505–550 nm.

Regarding the *HgSNARE1*-expressed transgenic Arabidopsis, at 35 dpi, the amount of females in the roots of each plant of the two transgenic lines were extremely less than that in wild-type Col-0 ($P < 0.001$), and the cysts in the roots and rhizosphere soils per plant of the two transgenic lines were also significantly decreased when compared to wild-type Col-0 (Fig. 2B). These results clearly indicate that expression of *HgSNARE1* enhanced the resistance of Arabidopsis to BCN, contrast to the function of *HsSNARE1* (Fig. 2A).

Subsequently, to further understand the reverse functions between HsSNARE1 and HgSNARE1 (Fig. 2A, B), their structures were modeled. In the whole protein sequences, the residues 64–305 in both HsSNARE1 and HgSNARE1 were modeled, covering from almost of the uncharacterized fragment in the *N*-terminal to the whole *t*-SNARE domain, but excluding the TM domain. Obviously, two regions display differences between them from the modeled structures as arrows directed in Fig. 2C, the details are shown in Fig. 2D. The first different region (red arrows directed) is located at the residues 141 to 149, and the 2nd different region (blue arrows directed) is located at the residues 198–225 (Fig. 2D). Within these two different regions, the structure of the second different region does not show obvious difference, whereas the structure of the first different region exhibits complete difference: a random coils structure is exhibited in HsSNARE1, while it is changed into an α-helixes structure in HgSNARE1, with three amino acid residues polymorphisms: E141D, A143T and -148S (Fig. 2D).

We hypothesized that the structure alterations between random coils and α-helixes might play an important role in mediating the shifts of functions of HsSNAER1 and HgSANRE1. Hence, we constructed a mutant of *HsSNARE1*, *HsSNARE1-M1*, using the cDNA sequences of *HgSNARE1* flanking the region encoding those three polymorphic amino acid residues (E141D, A143T and -148S) in the α-helixes to replace the corresponding sequences in the random coils of *HsSNARE1* (Fig. 2E). Then, the *HsSNARE1-M1* was induced into Arabidopsis Col-0 to generate the transgenic lines (Figure S7C). At 20 dpi of BCN, the females in two homozygous *HsSNARE1-M1*-expressed transgenic lines (HsSNARE1-M1-1 and HsSNARE1-M1-2) were exceptionally decreased when compared to wild-type Col-0 ($P < 0.0001$, Fig. 2F). At 35 dpi, compared to wild-type Col-0, both females and cysts in both transgenic lines were also significantly reduced ($P < 0.01$ at least, Fig. 2G). Thus, similar to *HgSNARE1*-expressed Arabidopsis plants (Fig. 2B), the resistance of *HsSNARE1-M1*-expressed Arabidopsis plants to BCN was significantly boosted. It could therefore be concluded that the mutations of the three polymorphic amino acid residues (E141D, A143T and -148S) caused the regional structure alteration and consequently, loss-of-function of *HsSNARE1* was occurred in Arabidopsis while infected with BCN.

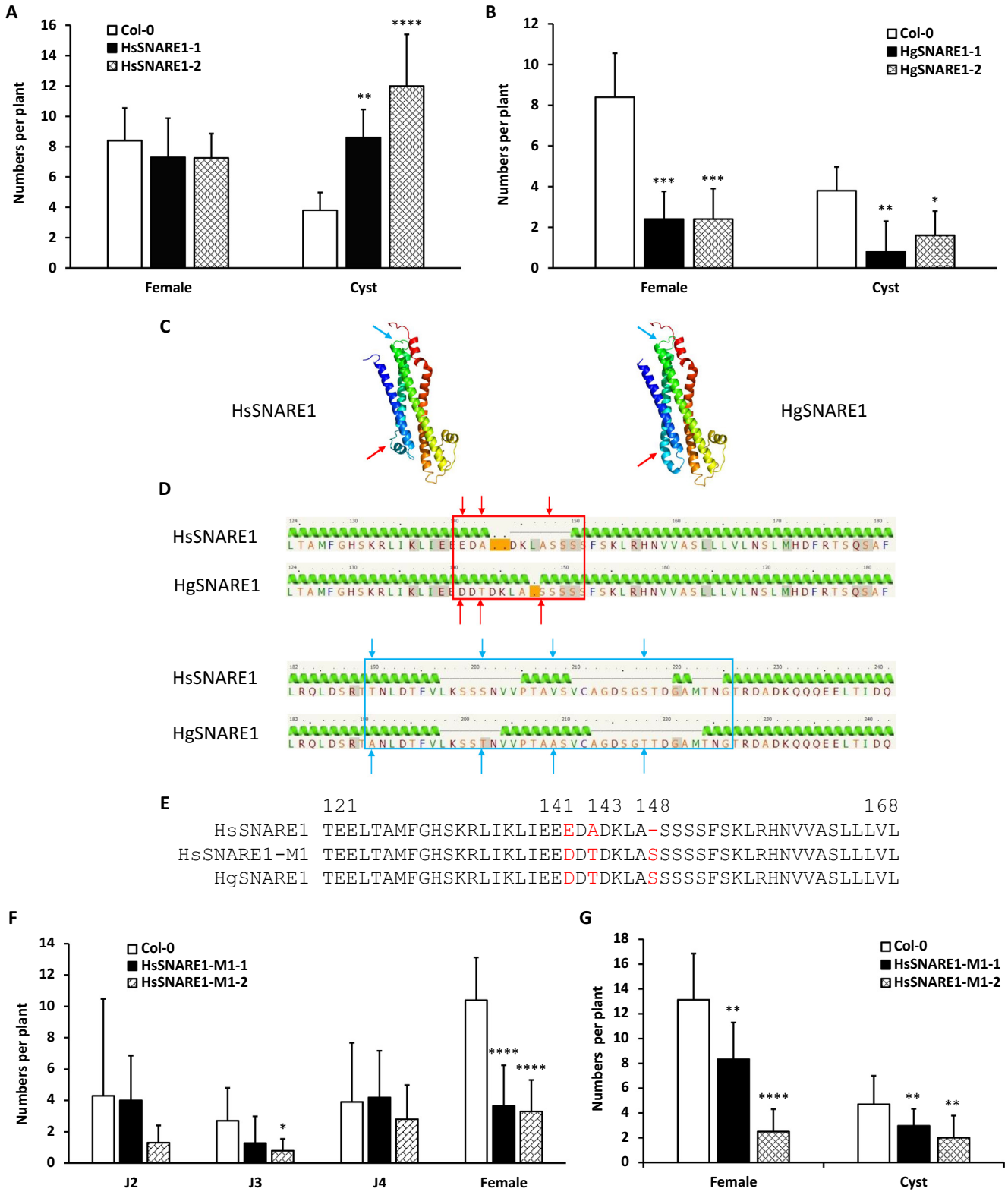

Fig. 2. Effects of expression of *HsSNARE1*, *HgSNARE1* and *HsSNARE1-M1* on the susceptibility of Arabidopsis to BCN. (A) and (B) Effects of expression of *HsSNARE1* (A) and *HgSNARE1* (B) on BCN susceptibility of Arabidopsis. (C) The modeled structures of HsSNARE1 and HgSNARE1 by Phyre 2. The arrows in red and blue show the two main different structures between HsSNARE1 and HgSNARE1. The red arrow-directed structures are random coils in HsSNARE1 and α-helixes in HgSNARE1. (D) The details of the two major different structures between HsSNARE1 and HgSNARE1. What the red and blue rectangles directed corresponds with what the red and blue arrows directed in (C), respectively. The arrows indicate the amino acid residues polymorphisms. (E) Construction of *HsSNARE1* mutant (*HsSNARE1-M1*). *HsSNARE1-M1* is identical with *HsSNARE1* except with the three red amino acid residues replacement of corresponding fragment of *HgSNARE1* at the random coils structure (E141D, A143T, and −148S). (F) and (G) Effects of expression of *HsSNARE1-M1* on BCN susceptibility of Arabidopsis. Col-0, wild-type Col-0. HsSNARE1-1 and HsSNARE1-2, HgSNARE1-1 and HgSNARE1-2, and HsSNARE1-M1-1 and HsSNARE1-M1-2 represent the identified two homozygous transgenic lines expressed with *HsSNARE1*, *HgSNARE1* and *HsSNARE1-M1*, respectively. Data show mean ± SE. The asterisk (*) denotes the significant difference in the numbers of BCN in the transgenic lines compared to the wild-type Col-0 analyzed by one-way ANOVA (*, $P < 0.05$; **, $P < 0.01$; ***, $P < 0.001$; ****, $P < 0.0001$). The experiments were replicated thrice with 6–10 replicates (plants) each time. The similar trends were shown each time. (For interpretation of the references to color in this figure legend, the reader is referred to the web version of this article.)

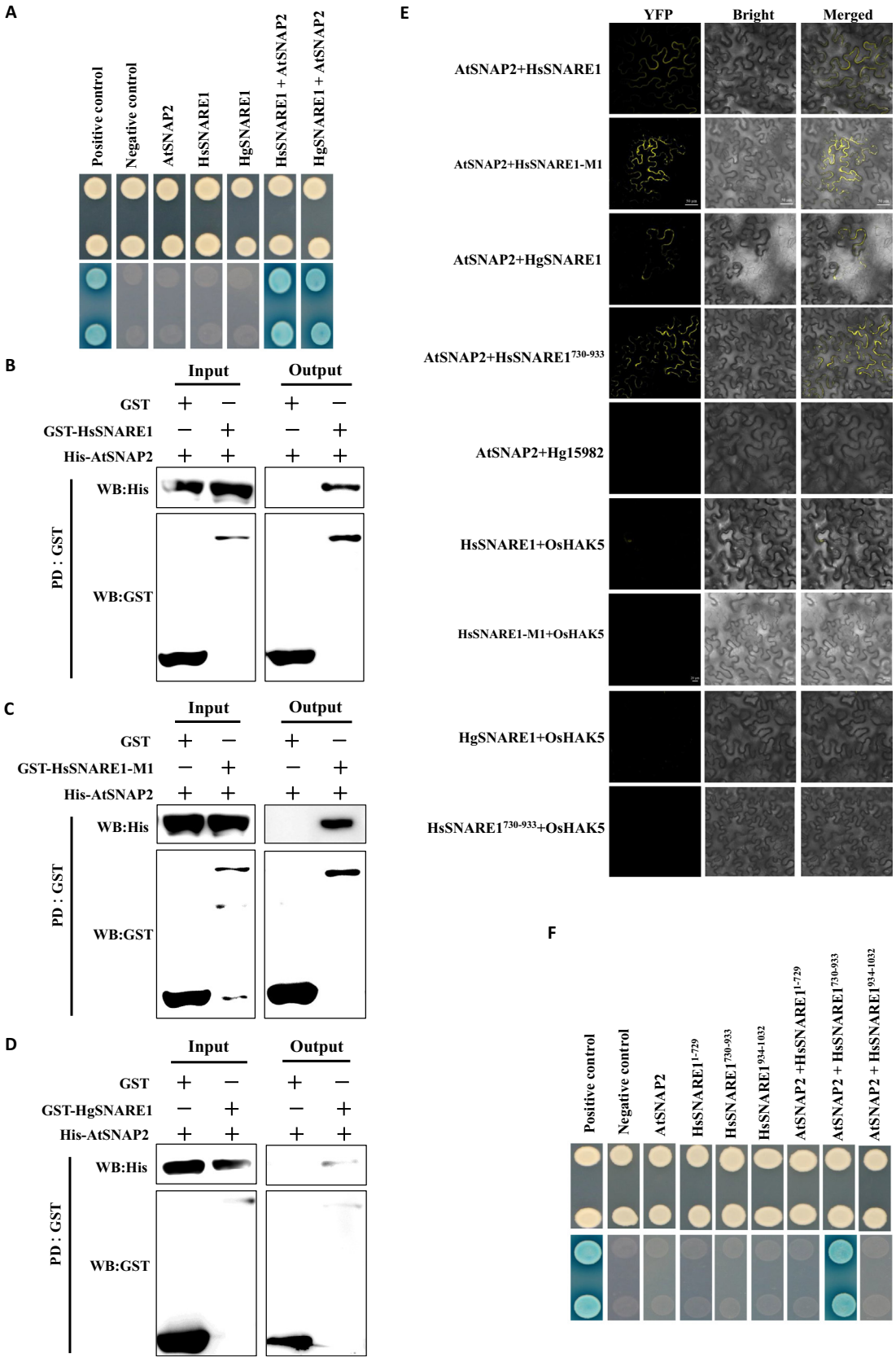

Fig. 3. Interactions of HsSNARE1, HsSNARE1-M1, HgSNARE1 and the *t*-SNARE domain with AtSNAP2. (A) Interactions of HsSNARE1 and HgSNARE1 with AtSNAP2 by yeast two hybrid assay. (B)-(D) Interactions of HsSNARE1, HsSNARE1-M1 and HgSNARE1 with AtSNAP2 by pulldown assay. GST and His are the tags. PD, pulldown; WB, western blotting. (E) Interactions of HsSNARE1, HsSNARE1-M1, HgSNARE1 and the *t*-SNARE domain (HsSNARE1$^{730-933}$) with AtSNAP2 by BiFC assay. AtSNAP2 + Hg15982 (Hetgly. T000015982.1), HsSNARE1 + OsHAK5 (Os01g0930400), HsSNARE1-M1 + OsHAK5, HgSNARE1 + OsHAK5, and HsSNARE1$^{730-933}$ + OsHAK5 were used as the negative controls. (F) Interactions of each part of HsSNARE1 with AtSNAP2 by yeast two hybrid assay. HsSNARE1$^{1-729}$, HsSNARE1$^{730-933}$ and HsSNARE1$^{934-1032}$ represent uncharacterized fragment, *t*-SNARE domain and transmembrane domain region, respectively.

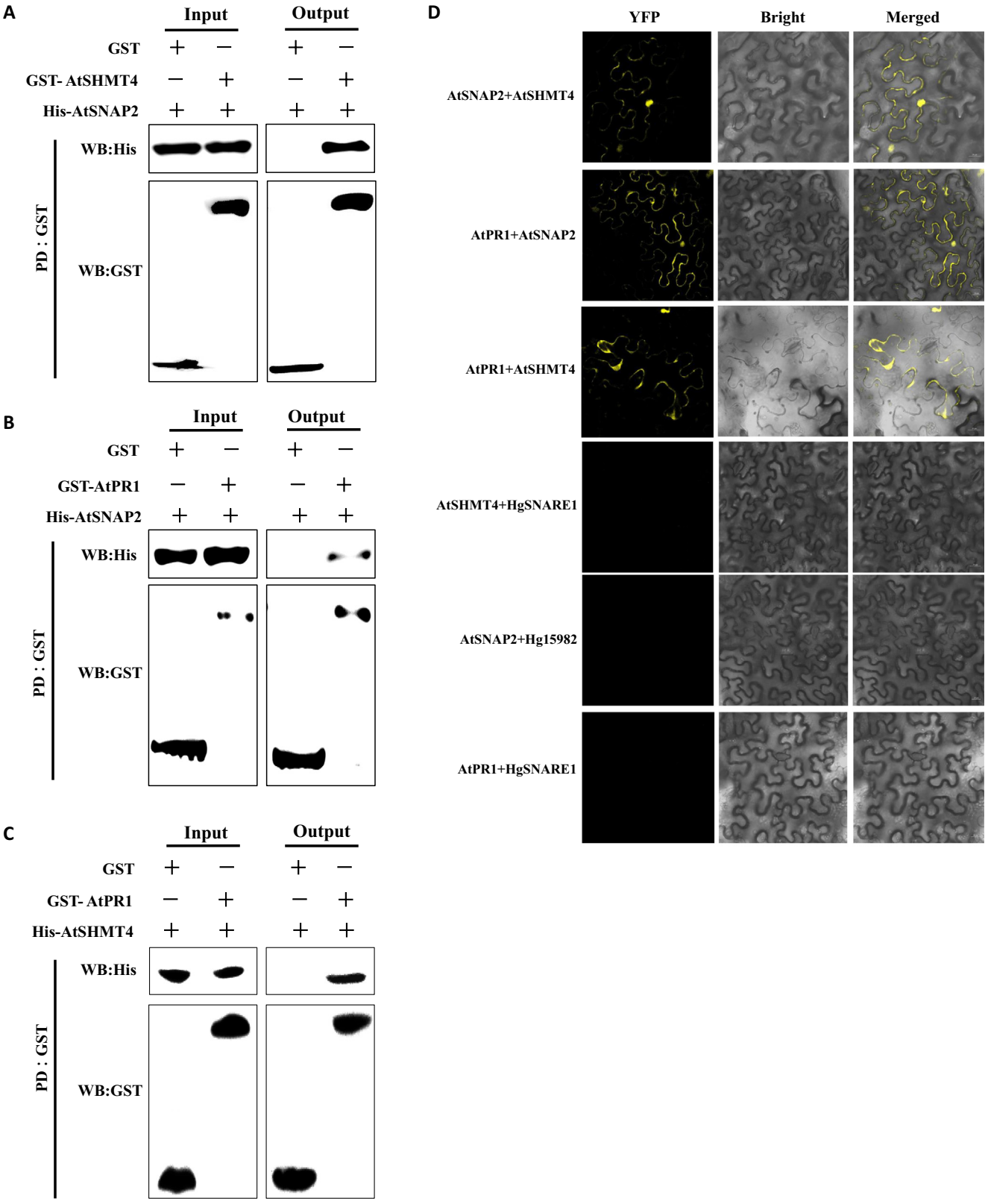

Fig. 4. Pairwise interactions among AtSNAP2, AtSHMT4 and AtPR1. (A)-(C) Interactions between AtSNAP2 and AtSHMT4, between AtSNAP2 and AtPR1, and between AtSHMT4 and AtPR1, respectively, by pulldown assay. GST and His are the tags. PD, pulldown; WB, western blotting. (D) Interactions between AtSNAP2 and AtSHMT4, between AtSNAP2 and AtPR1, and between AtSHMT4 and AtPR1, respectively, by BiFC assay. AtSHMT4 + HgSNARE1, AtSNAP2 + Hg15982 (Hetgly.T000015982.1), and AtPR1 + HgSNARE1 were used as the negative controls.

Interactions of HsSNARE1 and HgSNARE1 with AtSNAP2

A *t*-SNARE SCN protein HgSLP-1 could interact with soybean *rhg1-a* GmSNAP18 (Glyma.18 g022500, Peking-type *rhg1* GmSNAP18, [38]) [27]. Three SNARE soybean syntaxins all could bind *rhg1-b* α-SNAP (PI 88788-type *rhg1* GmSNAP18, [39]) [25,26]. By yeast two hybrid, we tested for the interactions of HgSNARE1 and HsSNARE1 with AtSNAP2 (At3g51690), which is highest similar to *rhg1-a* GmSNAP18 (GenBank Acc. No. KX147332) in Arabidopsis (75.1 %) [40]. The results show that both

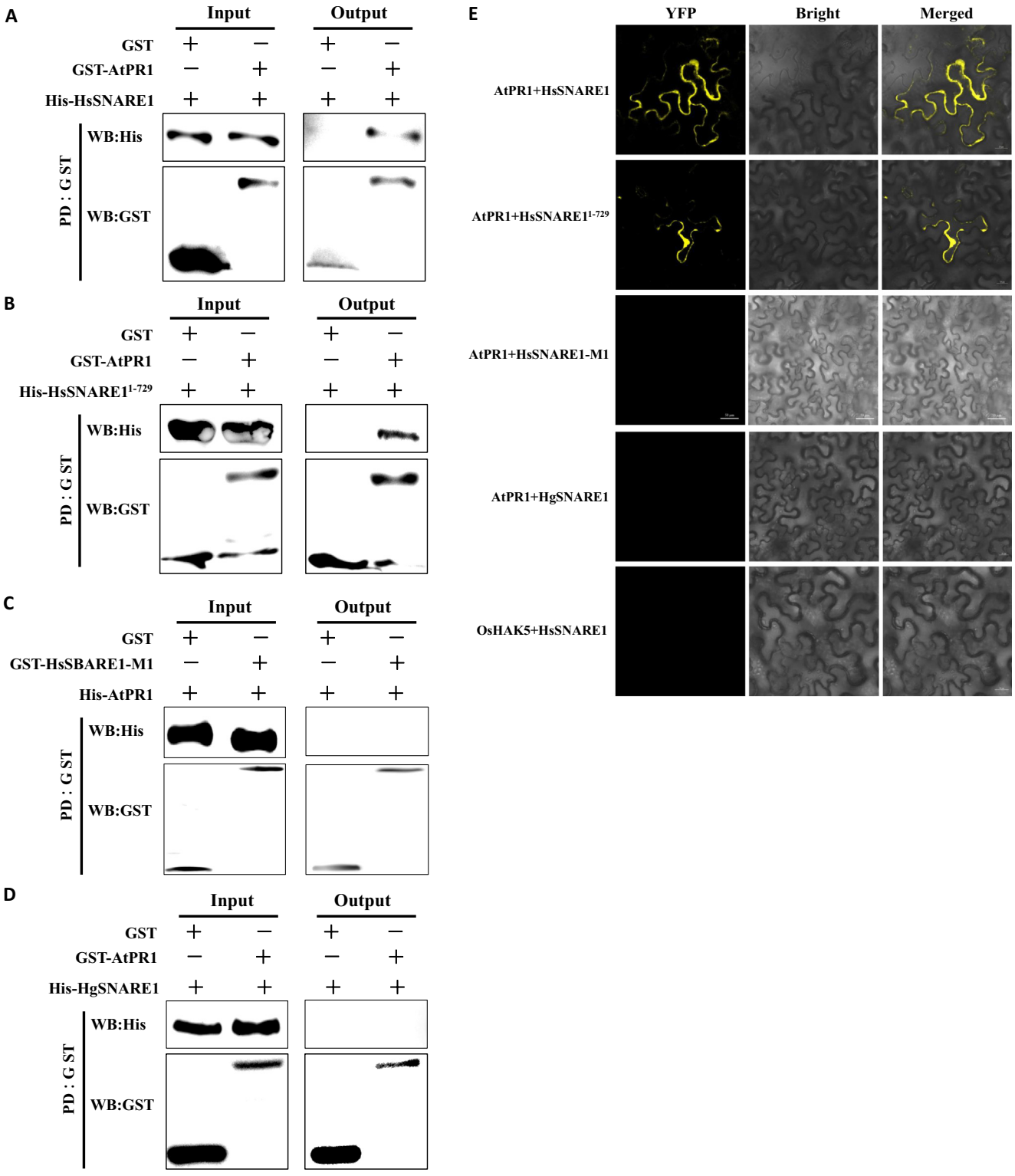

Fig. 5. Interactions of HsSNARE1, HsSNARE1$^{1-729}$, HsSNARE1-M1 and HgSNARE1 with AtPR1. (A)-(D) Interactions of HsSNARE1 and HsSNARE1$^{1-729}$, HsSNARE1-M1 and HgSNARE1 with AtPR1 by pulldown assay. GST and His are the tags. PD, pulldown; WB, western blotting. (E) Interactions of HsSNARE1, HsSNARE1$^{1-729}$, HsSNARE1-M1 and HgSNARE1 with AtPR1 by BiFC assay. OsHAK5 (Os01g0930400) + HsSNARE1 was used as the negative control. HsSNARE1$^{1-729}$ represents uncharacterized fragment in the *N*-terminal of HsSNARE1.

exhibited interactions with AtSNAP2 (Fig. 3A). Both pulldown (Fig. 3B-D) and bimolecular fluorescence complementation (BiFC, Fig. 3E) assays showed the interactions of HsSNARE1, HsSNARE1-M1 and HgSNARE1 with AtSNAP2.

To analyze which domain (fragment) is responsible for the interactions of HsNSARE1, HsSNARE1-M1 and HgSNARE1 with AtSNAP2, on the basis of the gene (cDNA) structures of *HsSNARE1* and *HgSNARE1* (Figure S3), different plasmids containing various fragments of *HsSNARE1* were constructed. The yeast two hybrid results indicated that only the *t*-SNARE domain (HsSNARE1$^{730\text{-}933}$), which is identical among HsSNARE1, HsSNARE1-M1 and HgSNARE1 (Figures S3, 2E), could interact with AtSNAP2 (Fig. 3E, F), indicating that the *t*-SNARE domain is responsible for the interactions of HsSNARE1, HsSNARE1-M1 and HgSNARE1 with AtSNAP2.

Pairwise interactions among AtSNAP2, AtSHMT4 and AtPR1

In soybean, *rhg1-a* GmSNAP18, *Rhg4* GmSHMT08 (Glyma.08 g108900, [41]) and GmPR08-Bet VI (Glyma.08 g230500) pairwise interacted for the resistance of Peking-type soybean to SCN [42]. We blasted and gained the orthologous Arabidopsis gene of *Rhg4* GmSHMT08 (GenBank Acc. No. JQ714080), AtSHMT4 (At4g13930), with the highest similarity (88.7 %) [40]. Subsequently, AtSNAP2, AtSHMT4 and the Arabidopsis pathogenesis-related protein AtPR1 (At2g14610) were tested for the interactions. The results of both pulldown and BiFC assays showed that the interactions occurred between AtSNAP2 and AtSHMT4, between AtSNAP2 and AtPR1, and between AtSHMT4 and AtPR1 (Fig. 4), indicating the pairwise interactions among AtSNAP2, AtSHMT4 and AtPR1. However, the homolog of AtPR1, AtPR5 (At1g75040) could interact neither AtSNAP2 nor AtSHMT4 (Figure S8).

No interactions of HsSNARE1 and HgSNARE1 with AtSHMT4

Subsequently, the interaction relationships of HsSNARE1, HsSNARE1-M1 and HgSNARE1 with AtSHMT4 were tested. The pulldown assay results showed that none of HsSNARE1, HsSNARE1-M1, and HgSNARE1 could interact with AtSHMT4 (Figure S9A-C). The BiFC assay further validated no interactions of HsSNARE1, HsSNARE1-M1 and HgSNARE1 with AtSHMT4 (Figure S9D).

Interaction of HsSNARE1 rather than HgSNARE1 with AtPR1

The pulldown assay results showed that HsSNARE1 and HsSNARE1$^{1\text{-}729}$ (*N*-terminal uncharacterized fragment) could interact with AtPR1, while neither HsSNARE1-M1 nor HgSNARE1 could interact with AtPR1 (Fig. 5A-D). These interactions were confirmed by BiFC assay (Fig. 5E). Together with the interactions of HsSNARE1, HsSNARE1-M1 and HgSANRE1 with AtSNAP2 (Fig. 3), we can conclude that HsSNARE1, HsSNARE1-M1 and HgSNARE1 all could interact with AtSNAP2 through the *t*-SNARE domain, but HsSNARE1 rather than HsSNARE1-M1 or HgSNARE1 could still

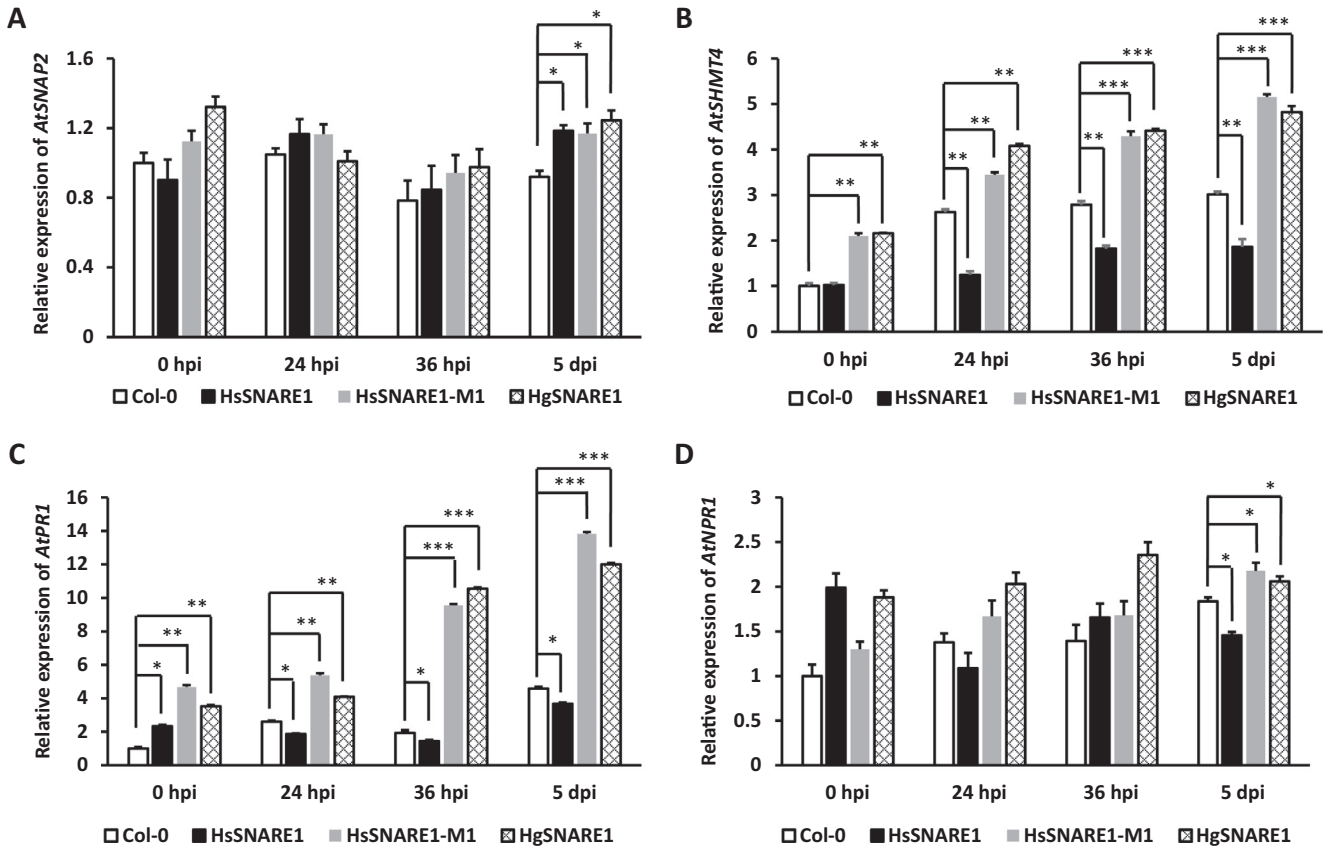

Fig. 6. Expression patterns of *AtSNAP2*, *AtSHMT4*, *AtPR1* and *AtNPR1* in the transgenic Arabidopsis expressing *HsSNARE1*, *HsSNARE1-M1* or *HgSNARE1* with the infection of BCN. (A)-(D) Expression patterns of *AtSNAP2*, *AtSHMT4*, *AtPR1* and *AtNPR1* in the transgenic Arabidopsis expressing *HsSNARE1*, *HsSNARE1-M1* or *HgSNARE1* with the infection of BCN, respectively. Col-0, HsSNARE1, HsSNARE1-M1 and HgSNARE1 represent wild-type Arabidopsis Col-0, *HsSNARE1*-expressed transgenic plant HsSNARE1-2, *HsSNARE1-M1*-expressed transgenic plant HsSNARE1-M1-2 and *HgSNARE1*-expressed transgenic plant HgSNARE1-1, respectively. All data show expression level relative to wild-type Col-0 at 0 hpi. *AtActin* was used as the reference gene. The experiments were performed thrice with triplicates each time, and the similar trends were obtained each time. The significant difference was statistically analyzed by one-way ANOVA (*, $P < 0.05$; **, $P < 0.01$; ***. $P < 0.001$).

interact with AtPR1 through the *N*-terminal uncharacterized fragment. Because only 3 amino acid residues polymorphisms (E141D, A143T and -148S) in the uncharacterized fragment in the *N*-terminal exist between HsSNARE1 and its mutant HsSNARE1-M1 (Fig. 2E), the *N*-terminal uncharacterized fragment of HsSNARE1 was responsible and the E^{141} and A^{143} amino acid residues and deletion of the 148th amino acid residue were essential, for the interaction between HsSNARE1 and AtPR1. Therefore, the SNARE domain interacts with AtSNAP2 (Fig. 3E, F), while the *N*-terminal uncharacterized fragment interacts with AtPR1, in HsSNARE1.

Opposite expression patterns of AtSHMT4 and AtPR1 between HsSNARE1- and HgSNARE1-expressed Arabidopsis infected with BCN

To further dissect the mechanism about the different functions of HsSNARE1, HsSNARE1-M1, and HgSNARE1 in Arabidopsis (Fig. 2), we measured the expression patterns of *AtSNAP2*, *AtSHMT4*, and *AtPR1* in the transgenic Arabidopsis with the infection of BCN. Additionally, expression of *AtNPR1*, which is a key regulatory gene in salicylic acid (SA) signaling pathway mediating *AtPR1*, was also measured. At 5 dpi, *AtSNAP2* was significantly induced in all *HsSNARE1*-, *HsSNARE1-M1*- and *HgSNARE1*-expressed Arabidopsis when compared to the wild-type (Fig. 6A). *AtSHMT4* was ominously suppressed in *HsSNARE1*-expressed Arabidopsis, in contrast, *AtSHMT4* was significantly induced in both *HsSNARE1-M1*- and *HgSNARE1*-expressed Arabidopsis after infected with BCN when compared to the wild-type (Fig. 6B). Similar to *AtSHMT4*, expression of *AtPR1* was also remarkably inhibited in *HsSNARE1*-expressed Arabidopsis but significantly enhanced in both *HsSNARE1-M1*- and *HgSNARE1*-expressed Arabidopsis before and after infected with SCN when compared to the wild-type (Fig. 6C). Regarding *AtNPR1*, it was suppressed in *HsSNARE1*-expressed Arabidopsis while boosted in both *HsSNARE1-M1*- and *HgSNARE1*-expressed Arabidopsis at 5 dpi when compared to the wild-type (Fig. 6D). These results indicate that both *AtSHMT4* and *AtPR1* exhibited opposite expression patterns between *HsSNARE1*-expressed Arabidopsis and *HsSNARE1-M1/HgSNARE1*-expressed Arabidopsis with infection of BCN. Due to the reverse functions of *HsSNARE1* and *HsSNARE1-M1/HgSNARE1* in the parasitism of BCN (Fig. 2A, B, F, G), and significant enhancement of the BCN resistance of Arabidopsis by overexpression of *AtSHMT4* [40], clearly, *AtSHMT4* negatively mediates BCN susceptibility of Arabidopsis that is positively regulated by HsSNARE1.

Enhancement of BCN resistance of Arabidopsis by overexpression of AtPR1

Based on the opposite expression patterns of *AtPR1* between *HsSNARE1*- and *HgSNARE1*/*HsSNARE1-M1*-expressed Arabidopsis (Fig. 6C), *AtPR1* is likely associated with the BCN susceptibility of Arabidopsis positively mediated by HsSNARE1. To validate the involvement of *AtPR1* in negatively mediating the susceptibility of Arabidopsis to BCN, we transformed and induced *AtPR1* into Arabidopsis, and the obtained homozygous T2 transgenic plants (Figure S7D) were inoculated with BCN. The females and cysts were

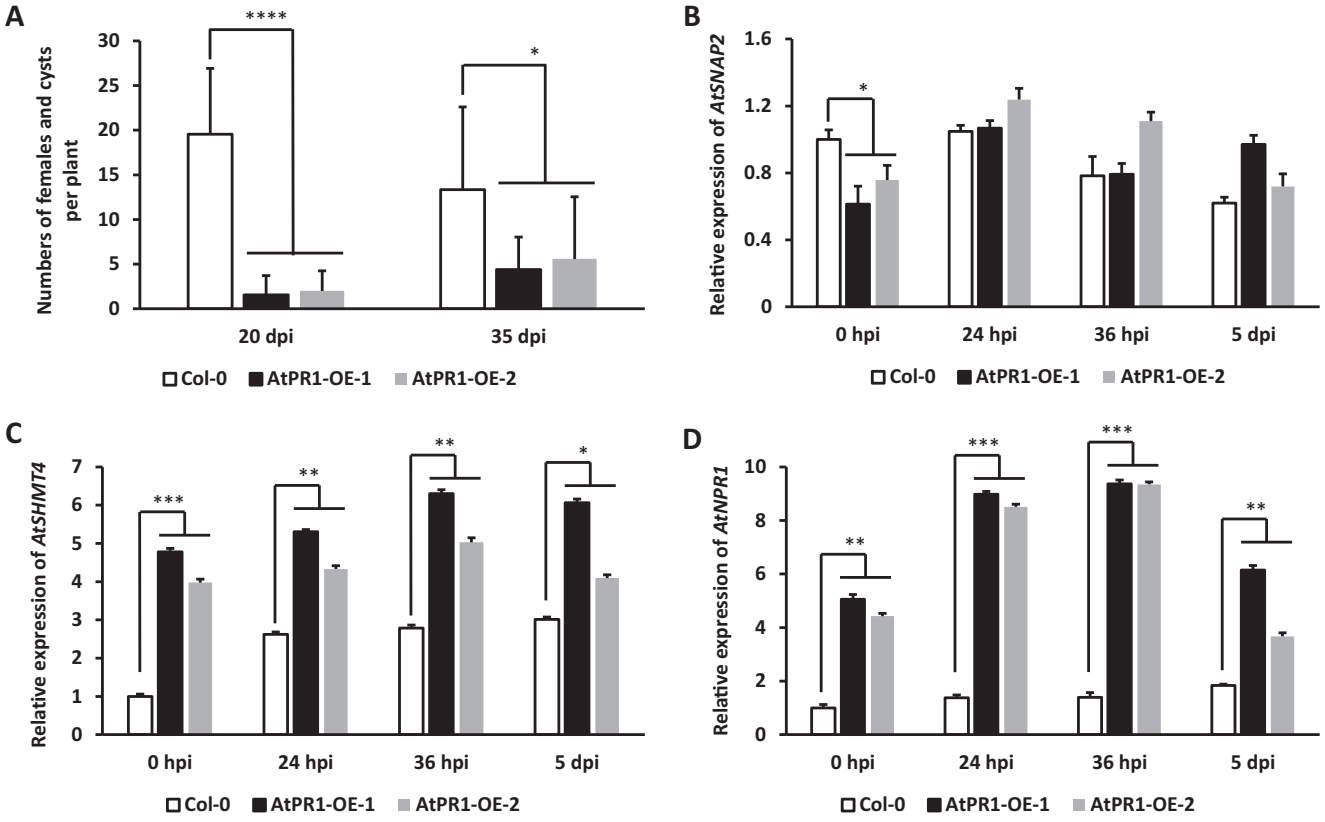

Fig. 7. BCN-infection phenotype of and expression patterns of *AtSNAP2*, *AtSHMT4* and *AtNPR1* in *AtPR1*-overexpressed transgenic Arabidopsis. (A) BCN-infection phenotype of *AtPR1*-overexpressed transgenic Arabidopsis. (B)-(D) Expression patterns of *AtSNAP2*, *AtSHMT4* and *AtNPR1* in *AtPR1*-overexpressed transgenic Arabidopsis with the infection of BCN, respectively. Col-0, AtPR1-OE-1 and AtPR1-OE-2 represent wild-type Arabidopsis Col-0, and two *AtPR1*-overexpressed homozygous transgenic plants, respectively. All data show expression level relative to wild-type Col-0 at 0 hpi. *AtActin* was used as the reference gene. The phenotyping experiments were conducted thrice with at least 10 replicates (plants) each line each time, the qRT-PCR experiments were performed thrice with triplicates each time, and the similar trends were obtained each time. The significant difference was statistically analyzed by one-way ANOVA (*, $P < 0.05$; **, $P < 0.01$; ***. $P < 0.001$; ****, $P < 0.0001$).

significantly reduced in the transgenic plants overexpressed with *AtPR1* at both 20 and 35 dpi when compared to the wild-type (Fig. 7A). These results show that overexpression of *AtPR1* significantly enhanced BCN resistance of Arabidopsis, similar to the reactions of *GmPR08-Bet VI*-expressed transgenic soybean to the SCN infection [42]. Combined with the different expression patterns of *AtPR1* in *HsSNARE1*-, *HsSNARE1-M1*- and *HgSNARE1*-expressed transgenic plants (Fig. 6C), it could be concluded that like *AtSHMT4*, *AtPR1* also negatively regulates susceptibility of Arabidopsis to BCN positively mediated by HsSNARE1. The expression patterns of *AtSNAP2*, *AtSHMT4* and *AtNPR1* were measured using homozygous *AtPR1*-overexpressed Arabidopsis. The results show that both *AtSHMT4* and *AtNPR1* were significantly induced by overexpression of *AtPR1* before and after infection of BCN, but *AtSNAP2* was not when compared to the wild-type (Fig. 7B-D), suggesting that *AtPR1* stimulates expression of *AtSHMT4*, meanwhile, *AtPR1* also positively promotes expression of *AtNPR1* while mediated by AtNPR1 in the SA signaling pathway.

Discussion

In this study, a *t*-SNARE domain-containing BCN HsSNARE1 was identified to enhance BCN susceptibility of Arabidopsis by interacting with both a pathogenesis-related AtPR1 and AtSNAP2 through its *N*-terminal uncharacterized fragment and *t*-SNARE domain, respectively (Figs. 3, 5), and overexpression of *AtPR1* significantly enhanced BCN resistance of Arabidopsis (Fig. 7A). The pathogenesis-related (*PR*) gene is one of the marker genes in the salicylic acid (SA) signaling pathway, which is a very important pathway to mediate the resistance of plants to pathogens. *PR* genes are also involved in mediating the plant resistance to nematodes [42–45]. However, whether and how nematodes regulate plant *PR* genes in the parasitism remain unknown. Our experimental results obtained in this study reveal that neither the mutant HsSNARE1-M1 of HsSNARE1, which carries three mutations (E141D, A143T and -148S) (Fig. 2E), nor its highly homologous SCN HgSNARE1 could interact with AtPR1 (Fig. 5). Those three amino acid mutations (polymorphisms) cause regional structure alteration between random coils of HsSNARE1 and α-helixes of HgSNARE1/HsSNARE1-M1 in the uncharacterized fragment of *N*-terminal (Fig. 2C). Therefore, this regional structure change might result in no interaction of HsSNARE1-M1 with AtPR1. Based on the additional interaction relationships between the cyst nematode *t*-SNARE proteins with AtSNAP2 (Fig. 3) and with AtSHMT4 (Figure S9), and among AtPR1, AtSNAP2 and AtSHMT4 (Fig. 4), the difference between the actions of HsSNARE1 and HsSNARE1-M1/HgSNARE1 is that HsSNARE1 rather than HsSNARE1-M1 or HgSNARE1 could interact with AtPR1 in Arabidopsis. *AtPR1* was significantly suppressed in *HsSNARE1*-expressed Arabidopsis while remarkably induced in both *HsSNARE1-M1*- and *HgSNARE1*-expressed Arabidopsis (Fig. 6C). Thus, *AtPR1* negatively mediates BCN susceptibility of Arabidopsis positively regulated by HsSNARE1.

A serine hydroxymethyltransferase (SHMT) *Rhg4* GmSHMT08 together with *rhg1-a* GmSNAP18 simultaneously controls SCN

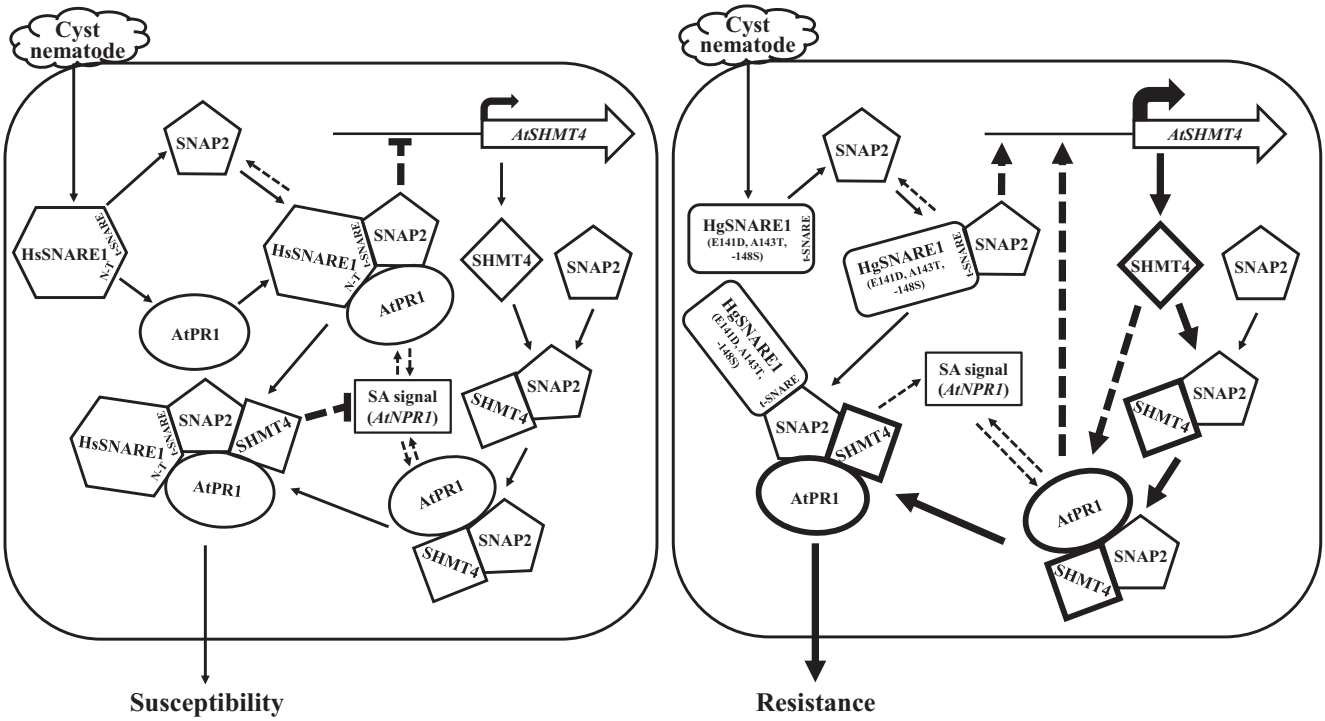

Fig. 8. A hypothesized model for *t*-SNARE cyst nematode proteins in Arabidopsis. In BCN parasitism, following secretion of the *t*-SNARE protein HsSNARE1 into root cells of Arabidopsis, HsSNARE1 interacts with AtSNAP2 through *t*-SNARE domain and AtPR1 through *N*-terminal uncharacterized fragment to form a complex, which inhibits expression of *AtSHMT4*, thus, AtSHMT4 is suppressed. AtSHMT4, AtSNAP2 and AtPR1 pairwise interact to form a complex, which then together with HsSNARE1-AtSNAP2-AtPR1 complex, forms a super HsSNARE1-AtSNAP2-AtSHMT4-AtPR1 complex. Meanwhile, AtNPR1 and AtPR1 can mutually mediate their expression through salicylic acid (SA) signaling pathway, however, *AtPR1* is significantly suppressed due to the interaction super-complex. In contrast, HgSNARE1 carrying three amino acid residue polymorphisms (E141D, A143T and −148S) from HsSNARE1 can interact with AtSNAP2 rather than AtPR1. The HgSNARE1-AtSNAP2 complex significantly induces expression of *AtSHMT4*, and then elevated AtSHMT4 stimulates expression of *AtPR1*. In the super HgSNARE1-AtSNAP2-AtSHMT4-AtPR1 complex, HgSNARE1 interacts with only AtSNAP2, and *AtPR1* is significantly induced. Therefore, the three amino acid residue polymorphisms in HgSNARE1 cause no interaction of *t*-SNARE proteins with AtPR1 but significant increase of expression of *AtSHMT4* and *AtPR1*. Resultantly, Arabidopsis shows susceptibility to BCN (compatible interaction) by HsSNARE1, while Arabidopsis displays resistance to BCN (incompatible interaction) by HgSNARE1. *t*-SNARE, *t*-SNARE domain. *N-T*, *N*-terminal uncharacterized fragment. SHMT4, AtSHMT4. SNAP2, AtSNAP2. Dotted lines and dotted *T*-shape lines denote up-regulation and down-regulation, respectively. Bold-highlighted rectangles and cycles denote boosted expression of the corresponding proteins.

resistance of Peking-type soybeans [38,41]. In this study, compared to the wild-type Col-0, *AtSHMT4* was significantly suppressed in *HsSNARE1*-expressed Arabidopsis (Fig. 6B), which showed enhanced susceptibility to BCN, while remarkably induced in both *HsSNARE1-M1*- and *HgSNARE1*-expressed Arabidopsis, both of which displayed boosted resistance to BCN (Fig. 2A, 2B, 2F, 2G). These results are consistent with the results of Zhao et al. [40] that *AtSHMT4* was suppressed in *GmSNAP18*-overexpressed Arabidopsis, which showed significantly enhanced BCN susceptibility when compared to the wild-type Arabidopsis, indicating the negative modulation of *AtSHMT4* in BCN susceptibility of Arabidopsis that is positively mediated by HsSNARE1.

AtSNAP2 was induced in all *HsSNARE1*-, *HsSNARE1-M1*- and *HgSNARE1*-expressed Arabidopsis at 5 dpi (Fig. 6A). Clearly, the opposite BCN-infection phenotypes of *HsSNARE1*- and *HsSNARE1-M1*/*HgSNARE1*-expressed transgenic Arabidopsis were not caused by the expression patterns of *AtSNAP2*. In soybean, GmSNAP18 induces expression (transcription) of *GmSHMT08* upon infection of SCN [42]. In Arabidopsis, the interactions among HsSNARE1, AtSNAP2 and AtPR1 (Figs. 3, 5) might suppress transcription of *AtSHMT4*, while interaction between HsSNARE1-M1/HgSNARE1 and AtSNAP2 (Fig. 3) likely promotes transcription of *AtSHMT4*. Additionally, overexpression of *AtPR1* significantly stimulated expression of *AtSHMT4* in Arabidopsis (Fig. 7C), and overexpression of *AtSHMT4* also ominously promoted expression of *AtPR1* in Arabidopsis [40]. So, AtPR1 and AtSHMT4 can positively mediate their expression in Arabidopsis mutually. AtNPR1 in the SA signaling pathway positively mediates expression of *AtPR1*. In this study, *AtNPR1* was inhibited in *HsSNARE1*-expressed Arabidopsis while significantly induced in both *HsSNARE1-M1*- and *HgSNARE1*-expressed Arabidopsis at 5 dpi (Fig. 6D), and overexpression of *AtPR1* stimulated expression of *AtNPR1* in Arabidopsis before and after infection of BCN (Fig. 7D). Therefore, AtPR1 and AtNPR1 can positively mediate their expression each other in Arabidopsis.

Plant nematode effectors play very important roles in the parasitism. Previously, an HgSLP-1 containing a *t*-SNARE domain was identified in SCN, but its effector functions were not characterized [27]. Recently, three SNARE soybean proteins were reported to bind *rhg1* α-SNAP and be involved in the mediation of *rhg1* resistance to SCN [25,26]. These reports suggest the importance of SNARE domain-containing genes in mediating nematode resistance. In this study, we isolated the *t*-SNARE domain-containing gene *HsSNARE1* from BCN (Figure S3). The transcripts of *HsSNARE1* was specifically accumulated in the subventral gland of BCN (Fig. 1A, 1B, S4, S5). Further analysis indicated that HsSNARE1 was secreted into cells of beet roots (Fig. 1D, S6). HsSNARE1 was therefore identified as a BCN effector.

Through these comparisons among HsSNARE1, HsSNARE1-M1 and HgSNARE1, a hypothesized model for actions of the *t*-SNARE cyst nematode proteins in Arabidopsis is summarized in Fig. 8. It can be concluded that the cyst nematode effector HsSNARE1 establishes nematode disease by directly interacting with both the pathogenesis-related AtPR1 through its *N*-terminal uncharacterized fragment and AtSNAP2 through its *t*-SNARE domain, and by significantly suppressing the *AtSHMT4* and *AtPR1* expression, in Arabidopsis. This is a new molecular mode of action of the SNARE domain-containing proteins, no matter in plant parasitic nematodes, or in plants, different from the previous reports about SNARE proteins [21,22,25].

Conclusions

In this study, a *t*-SNARE domain-containing BCN HsSNARE1 was identified as an effector, and its mutant HsSNARE1-M1 carrying three mutations (E141D, A143T and −148S) that altered regional structure from random coils to α-helixes was designed and constructed through protein structure modeling analysis between HsSNARE1 and its highly homologous HgSNARE1. Transgenic analyses demonstrated that expression of *HsSNARE1* ominously boosted while expression of *HgSNARE1*/*HsSNARE1-M1* fairly inhibited BCN susceptibility of Arabidopsis. Such opposite functions between HsSNARE1 and HgSNARE1 is caused by those three amino acid residue polymorphisms. HsSNARE1 promotes cyst nematode disease by directly targeting both AtSNAP2 and AtPR1 via its *t*-SNARE domain and *N*-terminal uncharacterized fragment, respectively, and remarkable suppression of both *AtSHMT4* and *AtPR1*. This work reveals a new molecular mode of action of the *t*-SNARE-domain containing cyst nematode effectors, providing a novel insight into interactions between cyst nematodes and host plants.

CRediT authorship contribution statement

S.L. conceived the project, designed the experiments, analyzed the data and wrote the manuscript. J.Z. performed the experiments and analyzed the data.

Data availability

The cDNA and predicted protein sequences of HgSNARE1 and HsSNARE1 were deposited on NCBI with GenBank Acc. Nos. of MN832862 and MN832863, respectively.

Declaration of Competing Interest

The authors declare that they have no known competing financial interests or personal relationships that could have appeared to influence the work reported in this paper.

Acknowledgements

This work was supported by the National Natural Science Foundation of China (31972248) and the Agricultral Science and Technology Innovation Program of Chinese Academy of Agricultural Sciences (ASTIP-02-IPP-04). The authors thank very much all the colleagues and other students in the lab for their valuable advice and comments, providing experimental materials, and their help and assistance in the experiments, especially, Drs. Deliang Peng and Huan Peng for supplying nematodes, and the graduate students Liuping Zhang, Zhi Liu and Ke Yao for their help in nematode-infection phenotyping, yeast two hybrid and in-situ hybridization. The authors appreciate the editing of Dr. Willibald Schliemann at Leibniz Institute of Plant Biochemistry, Germany and Dr. Wei Li at Hunan Agricultural University, China.

Appendix A. Supplementary data

Supplementary data to this article can be found online at https://doi.org/10.1016/j.jare.2022.07.004.

References

[1] Robertson L, Robertson WM, Sobczak M, Helder J, Tetaud E, Ariyanayagam MR, et al. Cloning, expression and functional characterisation of a peroxiredoxin from the potato cyst nematode *Globodera rostochiensis*. Mol Biochem Parasitol 2000;111(1):41–9. doi: https://doi.org/10.1016/s0166-6851(00)00295-4.

[2] Jones JT, Reavy B, Smant G, Prior AE. Glutathione peroxidases of the potato cyst nematode *Globodera rostochiensis*. Gene 2004;324:47–54. doi: https://doi.org/10.1016/j.gene.2003.09.051.

[3] Eves-van den AS, Lilley CJ, Jones JT, Urwin PE. Identification and characterisation of a hyper-variable apoplastic effector gene family of the potato cyst nematodes. PLoS Pathog 2014;10:. doi: https://doi.org/10.1371/journal.ppat.1004391e1004391.

[4] Le X, Wang X, Guan T, Ju Y, Li H. Isolation and characterization of a fatty acid- and retinoid-binding protein from the cereal cyst nematode *Heterodera avenae*. Exp Parasitol 2016;167:94–102. doi: https://doi.org/10.1016/j.exppara.2016.05.009.
[5] Hewezi T, Howe P, Maier TR, Hussey RS, Mitchum MG, Davis EL, Baum TJ. Cellulose binding protein from the parasitic nematode Heterodera schachtii interacts with Arabidopsis pectin methylesterase: cooperative cell wall modification during parasitism. Plant Cell 2008;20:3080–93. doi: https://doi.org/10.1105/tpc.108.063065.
[6] Lee C, Chronis D, Kenning C, Peret B, Hewezi T, Davis EL, Baum TJ, Hussey R, Bennett M, Mitchum MG. The novel cyst nematode effector protein 19C07 interacts with the Arabidopsis auxin influx transporter LAX3 to control feeding site development. Plant Physiol 2011;155:866–80. doi: https://doi.org/10.1104/pp.110.167197.
[7] Guo X, Wang J, Gardner M, Fukuda H, Kondo Y, Etchells JP, et al. Identification of cyst nematode B-type CLE peptides and modulation of the vascular stem cell pathway for feeding cell formation. PLoS Pathog 2017;13(2):e1006142. doi: https://doi.org/10.1371/journal.ppat.1006142.
[8] Hewezi T, Howe P, Maier TR, Hussey RS, Mitchum MG, Davis EL, Baumn TJ. Arabidopsis spermidine synthase is targeted by an effector protein of the cyst nematode Heterodera schachtii. Plant Physiol 2010;152:968–84. doi: https://doi.org/10.1104/pp.109.150557.
[9] Hamamouch N, Li C, Hewezi T, Baum TJ, Mitchum MG, Hussey RS, Vodkin LO, Davis EL. The interaction of the novel 30C02 cyst nematode effector protein with a plant β-1,3-endoglucanase may suppress host defence to promote parasitism. J Exp Bot 2012;63:3683–95. doi: https://doi.org/10.1093/jxb/ers058.
[10] Noon JB, Qi M, Sill DN, Muppirala U, Eves-van den Akker S, Maier TR, et al. A Plasmodium-like virulence effector of the soybean cyst nematode suppresses plant innate immunity. New Phytol 2016;212(2):444–60. doi: https://doi.org/10.1111/nph.14047.
[11] Barnes SN, Wram CL, Mitchum MG, Baum TJ. The plant-parasitic cyst nematode effector GLAND4 is a DNA-binding protein. Mol Plant Patholog 2018;19(10):2263–76. doi: https://doi.org/10.1111/mpp.12697.
[12] Siddique S, Radakovic ZS, De La Torre CM, Chronis D, Novák O, Ramireddy E, et al. A parasitic nematode releases cytokinin that controls cell division and orchestrates feeding site formation in host plants. Proc Natl Acad Sci USA 2015;112(41):12669–74. doi: https://doi.org/10.1073/pnas.1503657112.
[13] Hewezi T, Juvale PS, Piya S, Maier TR, Rambani A, Rice JH, Mitchum MG, Davis EL, Hussey RS, Baum TJ. The cyst nematode effector protein 10A07 targets and recruits host posttranslational machinery to mediate its nuclear trafficking and to promote parasitism in Arabidopsis. Plant Cell 2015;27:891–907. doi: https://doi.org/10.1105/tpc.114.135327.
[14] Pogorelko G, Juvale PS, Rutter WB, Hewezi T, Hussey R, Davis EL, et al. A cyst nematode effector binds to diverse plant proteins, increases nematode susceptibility and affects root morphology. Mol Plant Pathol 2016;17:832–44. doi: https://doi.org/10.1111/mpp.12330.
[15] Verma A, Lee C, Morriss S, Odu F, Kenning C, Rizzo N, et al. The novel cyst nematode effector protein 30D08 targets host nuclear functions to alter gene expression in feeding sites. New Phytol 2018;219(2):697–713. doi: https://doi.org/10.1111/nph.15179.
[16] Pogorelko GV, Juvale PS, Rutter WB, Hütten M, Maier TR, Hewezi T, et al. Re-targeting of a plant defense protease by a cyst nematode effector. Plant J 2019;98(6):1000–14. doi: https://doi.org/10.1111/tpj.14295.
[17] Wang J, Yeckel G, Kandoth PK, Wasala L, Hussey RS, Davis EL, et al. Targeted suppression of soybean BAG6-induced cell death in yeast by soybean cyst nematode effectors. Mol Plant Pathol 2020;21(9):1227–39. doi: https://doi.org/10.1111/mpp.12970.
[18] Jahn R, Scheller RH. SNAREs: engines for membrane fusion. Nat Rev Mol Cell Biol 2006;7(9):631–43. doi: https://doi.org/10.1038/nrm2002.
[19] Fasshauer D, Sutton RB, Brunger AT, Jahn R. Conserved structural features of the synaptic fusion complex: SNARE proteins reclassified as Q- and R-SNAREs. Proc Natl Acad Sci USA 1998;95(26):15781–6. doi: https://doi.org/10.1073/pnas.95.26.15781.
[20] Bock JB, Matern HT, Peden AA, Scheller RH. A genomic perspective on membrane compartment organization. Nature 2001;409(6822):839–41. doi: https://doi.org/10.1038/35057024.
[21] Jones AM, Xuan Y, Xu M, Wang R-S, Ho C-H, Lalonde S, et al. Border control-a membrane-linked interactome of Arabidopsis. Science 2014;344(6185):711–6. doi: https://doi.org/10.1126/science.1251358.
[22] Zhang L, Liu Y, Zhu XF, Jung JH, Sun Q, Li TY, et al. SYP22 and VAMP727 regulate BRI1 plasma membrane targeting to control plant growth in Arabidopsis. New Phytol 2019;223(3):1059–65. doi: https://doi.org/10.1111/nph.15759.
[23] Bayless AM, Smith JM, Song J, McMinn PH, Teillet A, August BK, et al. (2016) Disease resistance through impairment of alpha-SNAP-NSF interaction and vesicular trafficking by soybean *Rhg1*. Proc Natl Acad Sci USA 2016;113:E7375–82. doi: https://doi.org/10.1073/pnas.1610150113.
[24] Bayless AM, Zapotocny RW, Grunwald DJ, Amundson KK, Diers BW, Bent AF. An atypical N-ethylmaleimide sensitive factor enables the viability of nematode-resistant *Rhg1* soybeans. Proc Natl Acad Sci USA 2018;115:E4512–21. doi: https://doi.org/10.1073/pnas.1717070115.
[25] Dong J, Zielinski RE, Hudson ME. t-SNAREs bind the *Rhg1* α-SNAP and mediate soybean cyst nematode resistance. Plant J 2020;104(2):318–31. doi: https://doi.org/10.1111/tpj.14923.
[26] Wang R, Deng M, Yang C, Yu Q, Zhang L, Zhu Q, Guo X. A Qa-SNARE complex contributes to soybean cyst nematode resistance via regulation of mitochondria-mediated cell death. J Exp Bot 2021;72:7145–62. doi: https://doi.org/10.1093/jxb/erab301.
[27] Bekal S, Domier LL, Gonfa B, Lakhssassi N, Meksem K, Lambert KN, et al. A SNARE-like protein and biotin are implicated in soybean cyst nematode virulence. PLoS ONE 2015;10(12):e0145601.
[28] Ge F-Y, Zheng N, Zhang L-P, Huang W-K, Peng D-L, Liu S-M. Chemical mutagenesis and soybean mutants potential for identification of novel genes conferring resistance to soybean cyst nematode. J Integ Agr 2018;17(12):2734–44. doi: https://doi.org/10.1016/S2095-3119(18)62105-7.
[29] de Boer JM, Yan Y, Smant G, Davis EL, Baum TJ. *In-situ* hybridization to messenger RNA in *Heterodera glycines*. J Nematol 1998;30:309–12.
[30] Gao B, Allen R, Maier T, Davis EL, Baum TJ, Hussey RS. Molecular characterisation and expression of two venom allergen-like protein genes in *Heterodera glycines*. Intl J Parasitol 2001;31(14):1617–25. doi: https://doi.org/10.1016/s0020-7519(01)00300-9.
[31] Elling AA, Mitreva M, Recknor J, Gai X, Martin J, Maier TR, et al. Divergent evolution of arrested development in the dauer stage of *Caenorhabditis elegans* and the infective stage of *Heterodera glycines*. Genome Biol 2007;8(10):R211. doi: https://doi.org/10.1186/gb-2007-8-10-r211.
[32] Livak KJ, Schmittgen TD. Analysis of relative gene expression data using real-time quantitative PCR and the $2^{-\Delta\Delta CT}$ method. Methods 2001;25(4):402–8. doi: https://doi.org/10.1006/meth.2001.1262.
[33] Zhao J, Mejias J, Quentin M, Chen Y, Almeida-Engler J, Mao Z, et al. The root-knot nematode effector MiPDI1 targets a stress associated protein (SAP) to establish disease in Solanaceae and Arabidopsis. New Phytol 2020;228(4):1417–30. doi: https://doi.org/10.1111/nph.16745.
[34] Luo S, Liu S, Kong L, Peng H, Huang W, Jian H, et al. Two venom allergen-like proteins, HaVAP1 and HaVAP2, are involved in the parasitism of *Heterodera avenae*. Mol Plant Pathol 2019;20(4):471–84. doi: https://doi.org/10.1111/mpp.12768.
[35] Clough SJ, Bent AF. Floral dip: a simplified method for Agrobacterium-mediated transformation of *Arabidopsis thaliana*. Plant J 2001;16:735–43. doi: https://doi.org/10.1046/j.1365-313x.1998.00343.x.
[36] Zhang X, Peng H, Zhu S, Xing J, Li X, Zhu Z, et al. Nematode-encoded RALF peptide mimics facilitate parasitism of plants through the FERONIA receptor kinase. Mol Plant 2020;13(10):1434–54. doi: https://doi.org/10.1016/j.molp.2020.08.014.
[37] Masonbrink R, Maier TR, Muppirala U, Seetharam AS, Lord E, Juvale PS, et al. The genome of the soybean cyst nematode (*Heterodera glycines*) reveals complex patterns of duplications involved in the evolution of parasitism genes. BMC Genomics 2019;20(1). doi: https://doi.org/10.1186/s12864-019-5485-8.
[38] Liu S, Kandoth PK, Lakhssassi N, Kang J, Colantonio V, Heinz R, et al. The soybean *GmSNAP18* gene underlies two types of resistance to soybean cyst nematode. Nature Commun 2017;8(1). doi: https://doi.org/10.1038/ncomms14822.
[39] Cook DE, Lee TG, Guo X, Melito S, Wang K, Bayless AM, et al. Copy number variation of multiple genes at *Rhg1* mediates nematode resistance in soybean. Science 2012;338(6111):1206–9. doi: https://doi.org/10.1126/science.1228746.
[40] Zhao J, Duan Y, Kong L, Huang W, Peng H, Peng D, et al. Opposite beet cyst nematode-infection phenotypes of transgenic Arabidopsis between overexpressing *GmSNAP18* and *AtSNAP2* and between overexpressing *GmSHMT08* and *AtSHMT4*. Phytopathology 2022. doi: https://doi.org/10.1094/PHYTO-01-22-0011-R.
[41] Liu S, Kandoth PK, Warren SD, Yeckel G, Heinz R, Alden J, et al. A soybean cyst nematode resistance gene points to a new mechanism of plant resistance to pathogens. Nature 2012;492(7428):256–60. doi: https://doi.org/10.1038/nature11651.
[42] Lakhssassi N, Piya S, Bekal S, Liu S, Zhou Z, Bergounioux C, et al. A pathogenesis related protein GmPR10-08 promotes a molecular interaction between the GmSHMT08 and GmSNAP18 in resistance to SCN. Plant Biotechnol J 2020;18:1810–29. doi: https://doi.org/10.1111/pbi.13343.
[43] Uehara T, Sugiyama S, Matsuura H, Arie T, Masuta C. Resistant and susceptible responses in tomato to cyst nematode are differentially regulated by salicylic acid. Plant Cell Physiol 2010;51:1524–36. doi: https://doi.org/10.1093/pcp/pcq109.
[44] Matthews BF, Beard H, Brewer E, Kabir S, MacDonald MH, Youssef RM. Arabidopsis genes, *AtNPR1*, *AtTGA2* and *AtPR-5*, confer partial resistance to soybean cyst nematode (*Heterodera glycines*) when overexpressed in transgenic soybean roots. BMC Plant Biol 2014;14(1):96. doi: https://doi.org/10.1186/1471-2229-14-96.
[45] Chen J, Hu L, Sun L, Lin B, Huang K, Zhuo K, et al. A novel *Meloidogyne graminicola* effector, MgMO237, interacts with multiple host defence-related proteins to manipulate plant basal immunity and promote parasitism. Mol Plant Pathol 2018;19(8):1942–55. doi: https://doi.org/10.1111/mpp.12671.